FeS_2-modified MXene nanocomposite platform for efficient PTT/CDT/TDT integration through enhanced GSH consumption

Yunfeng Tang[1], Renliang Zhao[2], Min Yi[2], Zilu Ge[2], Dong Wang[2], Yu Jiang[1], Guanglin Wang[2], Xiangtian Deng[2#]

[1]Head & Neck Oncology Ward, Cancer Center, West China Hospital, Cancer Center, Sichuan University, Chengdu, China.

[2]Trauma medical center, Department of Orthopedics surgery, West China Hospital, Sichuan University, Chengdu 610041, China.

Disclosure statement

There are no conflicts of interest to declare.

Funding

Natural Science Foundation of Sichuan (2023NSFSC1835), Tibet Autonomous Region co-funded project (XZ202301ZY0046G), Post-Doctor Research Project of West China Hospital, Sichuan University (2023HXBH106), China Postdoctoral Science Foundation（2023M732467, 2023TQ0224）

Author contribution

Yunfeng Tang and Renliang Zhao equally contribution

Corresponding author

Correspondence to Xiangtian Deng.

A: Experimental Section

Synthesis of hollow mesoporous FeS_2

Hollow mesoporous FeS_2 nanoparticles were synthesized using a previously documented method with minor modifications [1]. In a standard synthesis, iron nitrate nonahydrate (0.01 moles, >98%, obtained from Sigma-Aldrich) was mixed with 1-butanol (0.12 moles), nitric acid (0.019 moles), and P123 surfactant (2×10^{-4} moles) in a 150 mL beaker. The mixture was stirred at room temperature until a transparent gel formed. This gel was then transferred to an oven and heated at 80 °C for 3 hours. After heating, the product was allowed to cool, washed four times with ethanol, and centrifuged. The resulting powder was left to dry overnight in a vacuum oven. Subsequently, the dried powder underwent calcination at 150 °C for 12 hours under ambient air conditions, transforming into meso-Fe_2O_3. The sulfurization experiments were conducted at atmospheric pressure and 250 °C. In each experiment, a quartz tubular reactor was loaded with 100 mg of the as-prepared amorphous iron oxide and 200 mg of sulfur powder. A helium gas leak check was performed before the sulfurization setup. A mixture of 1% H_2S in helium was then flowed through the sample at a rate of 47 cm^3 per minute. The temperature

of the sample was gradually increased at a rate of 1 °C/min until it reached 250 °C, and maintained at this temperature for 12 hours. Excess H_2S was removed by passing the exhaust gas through a lead nitrate solution. The final product obtained from this process was identified as meso- FeS_2.

Synthesis of AIPH-loaded FeS_2 NPs

A dispersion was prepared by combining 1 mg of FeS_2 with 5 mg of AIPH in 5 mL of deionized water (DI water). This mixture was stirred for 24 hours to fabricate FeS_2@AIPH (FA) nanoparticles. The solution was then centrifuged and washed three times with DI water to produce dispersed FA nanoparticles for subsequent experiments.To synthesize amino-modified FA using the reversed-phase microemulsion method, 25 μL of $NH_3 \cdot H_2O$ (25 wt%) was added to a 10 mg FeS_2 solution and allowed to stand for 40 minutes. In a separate container, 7.5 mL of cyclohexane, 1.8 mL of n-hexanol, and 1.8 mL of Triton X-100 were mixed evenly. The pre-incubated solution was then added along with 30μL of polydiallyldimethylammonium chloride (PDDA), and 80 μL of $NH_3 \cdot H_2O$ (25 wt%) to form a microemulsion. Subsequently, 100μl of tetraethyl orthosilicate (TEOS) was slowly added, and the mixture was stirred continuously for 24 hours. After this period, 10μl of 3-aminopropyltriethoxysilane (APTES) was added and the reaction continued for an additional 12 hours. To terminate the reaction, 20 mL of acetone was added to the reaction mixture, which was then centrifuged to obtain amino-modified FA nanoparticles. To determine the drug loading of FA, initially synthesized hollow FeS2 nanoparticles were dispersed in aqueous solutions containing various concentrations of AIPH and subjected to magnetic stirring at 30°C for 12 hours. The solution was then centrifuged at 12,000 rpm for 10 minutes to yield the FA nanoparticles, which were subsequently washed three times with deionized water to remove any residual AIPH. The loading content (LC) of AIPH was then computed using the formula [2]: LC_AIPH = (Weight of loaded AIPH / Weight of FeS_2 nanoparticles) x 100%.

Synthesis of Ti_3C_2/FeS_2 @BSA- AIPH Nanosheets

To synthesize Ti_3C_2/FeS_2 @BSA-AIPH (TFAB) nanosheets, the procedure was meticulously followed. Initially, 10 mL of a Ti_3C_2 nanosheet solution (concentration: 250 μg/mL) was added to 5 mL of an FA solution (concentration: 500 μg/mL). This mixture was stirred continuously at room temperature for four hours to form the Ti_3C_2/FeS_2-AIPH (TFA) solution. After the formation of the TFA solution, it was centrifuged to separate the solids, which were then washed with deionized water to remove impurities. Subsequently, 5 mL of the cleaned TFA solution was ultrasonically dispersed with 5 mL of a BSA solution (1 mg/mL) for ten minutes to ensure thorough mixing. Simultaneously, Sorbitan monooleate was added to 50 mL of liquid paraffin, and this mixture was stirred for two hours to achieve a homogeneous emulsion. This emulsion was then added to the BSA-containing TFA solution, and the resulting mixture was stirred at room temperature for an additional two hours. During this final stirring phase, 0.5 g of glutaraldehyde was introduced to cross-link the components. The resulting mixture was then centrifuged, the precipitate washed multiple times with deionized water, and finally, the TFAB nanosheets were dried using vacuum freeze-drying to yield the final product.

Characterization

Morphological analysis of nanoparticles (NPs) at each stage of preparation was carried out using Transmission Electron Microscopy (TEM, FEI Talos F200X, 200 kV). Elemental analysis was conducted through Energy-dispersive X-ray Spectroscopy (EDS), an accessory of the TEM. Dynamic Light Scattering (DLS) was performed with a Zetasizer Nano ZS90 (Malvern, UK) to ascertain hydrodynamic diameters and zeta potential of the NPs. For enhanced resolution, Scanning Electron Microscopy (SEM) was executed using a transmission electron microscope (ZEISS, Gemini 300). The crystalline structure was probed with X-ray Diffraction (XRD) employing an X-ray diffractometer (XRD-7000, Shimadzu). Chemical composition was assessed through X-ray Photoelectron Spectroscopy (XPS) utilizing an XPS spectrometer.

ESR Measurement

ESR was utilized spectroscopy to identify the types of free radicals generated by TFAB. In this process, α-(4-pyridyl N-oxide)-N-tert-butylnitrone (POBN, 100 mm) at a volume of 100 μL was integrated into a 5 mL TFAB aqueous dispersion contained in a centrifuge tube to trace the formation of alkyl free radicals. Following this, the solution was exposed to an 808 nm, 1.5 W cm^{-2} irradiation for varying durations. Subsequently, the ESR spectra were captured using an ESR spectrometer (EMXnano, Bruker, Germany).

Cellular uptake of TFAB

MNNG/HOS cells were cultured in 12-well plates at a seeding density of 5×10^4 cells per well. Following an overnight incubation at a constant temperature of 37 °C with 5 % CO2 to ensure complete attachment, the cells were treated with ICG-labeled NPs (designated as ICG@TFAB) for varying durations of 1, 2, 4, and 8 h. At each time point, the cells underwent washing and subsequent staining of the nuclei using DAPI. Following this, PBS was used for three wash cycles, and fluorescence microscopy (Olympus Corporation, Tokyo, Japan) was employed for imaging purposes.

Measurement of Mitochondrial Membrane Potential

Mitochondrial membrane potential analysis was conducted utilizing flow cytometry with JC-1 dye, following the assay kit guidelines. Briefly, subsequent to the treatments, cells were subjected to staining with a JC-1 working buffer for 20 minutes within a 37°C incubator. Following this, the cells were harvested, underwent centrifugation, and were resuspended in the incubation medium. Fluorescence intensity measurements were carried out using a fluorescence spectroscopy instrument (F-2700 Techcomp (China) Ltd.). The relative mitochondrial membrane potential was assessed by calculating the red/green fluorescence intensity ratio, adhering to established research practices.

Animal tumor model establishment

Animal experiments were performed in accordance with the Guide for the Care and Use of Laboratory Animals and were approved by Institutional Animal Care and Use Committee of Sichuan University. MNNG/HOS tumor bearing Balb/c nude mice were chosen as the animal tumor models in this study. In brief, 200 μl of PBS containing MNNG/HOS cells (1×10^7) was subcutaneously injected into right flank of Balb/c mice. Subsequently, the animal tumor model was continuously bred when the tumor volume reached nearly 80-100 mm^3

B: Supplementary Figures

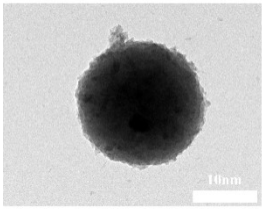

Figure S1 TEM images of mesoporous FeS_2 NPs.

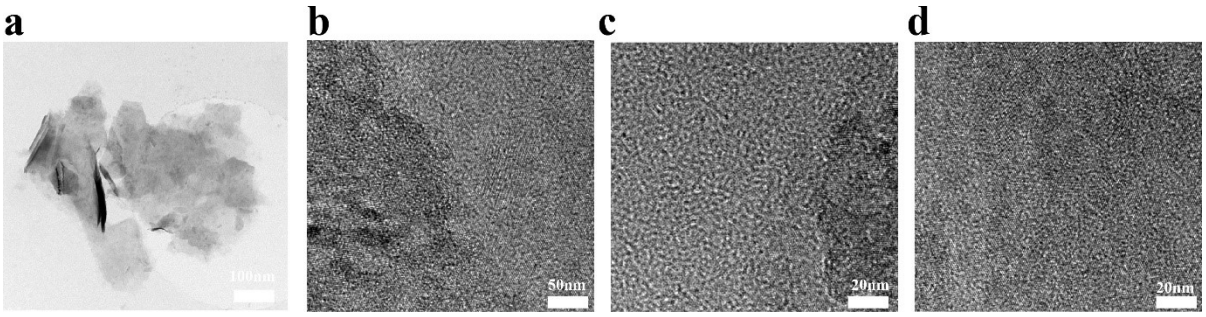

Figure S2 TEM image of single- or few-layer Ti_3C_2 after TPOAH intercalation.

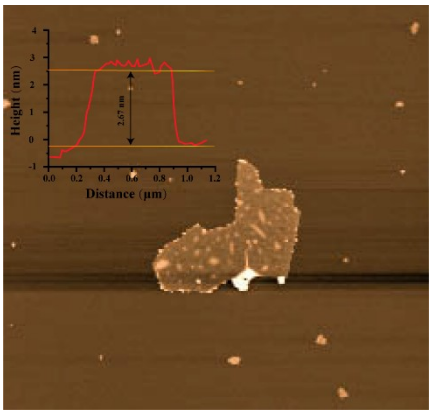

Figure S3 The thickness of Ti_3C_2 was measured by atomic force microscopy (AFM).

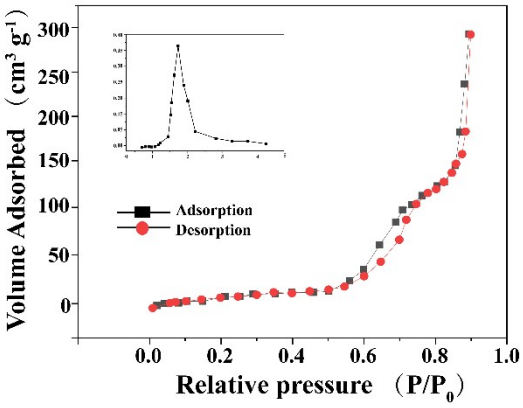

Figure S4 N_2 adsorption/desorption isotherms and pore-size distribution curve of the as-synthesized mesoporous FeS_2 NPs.

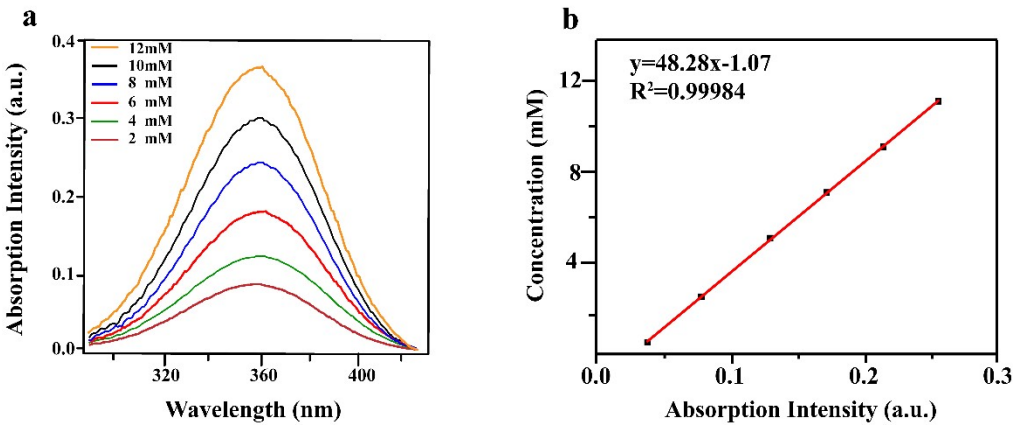

Figure S5 a) Standard absorbance curve of AIPH. b) The absorbance of AIPH molecules at 364nm (from water) as a function of AIPH concentration.

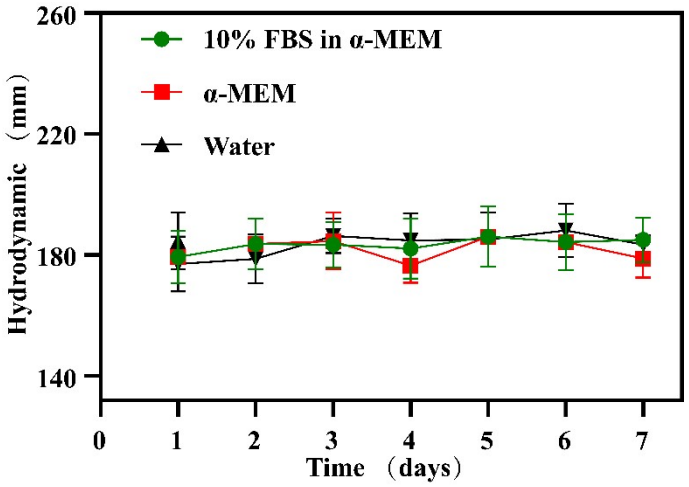

Figure S6 The hydrodynamic size changes of TFAB in various aqueous conditions, including water, a-MEM culture medium with or without 10 % FBS for 7 days.

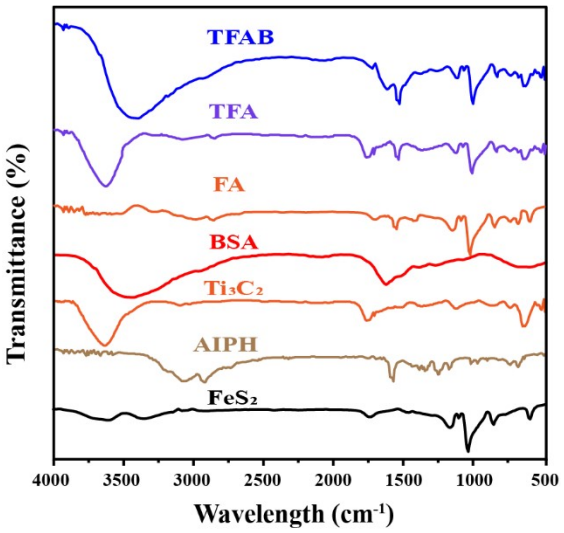

Figure S7: Comparative FTIR spectra of TFAB, TFA, FA, BSA, Ti_3C_2, AIPH and FeS_2

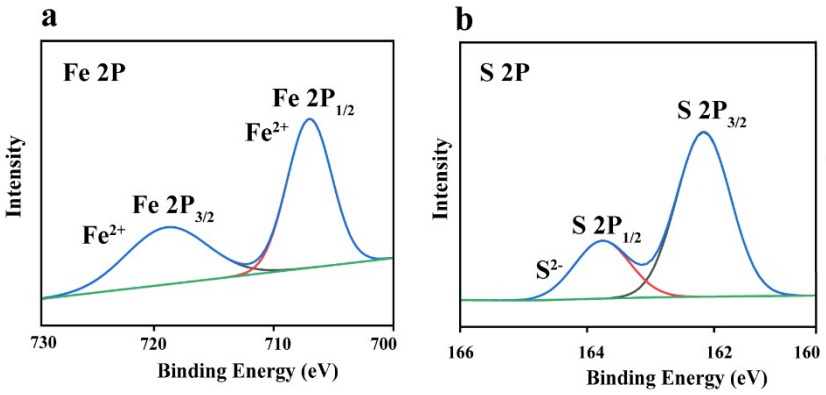

Figure S8 XPS spectra of S 2p and Fe 2p of the TFAB NPs.

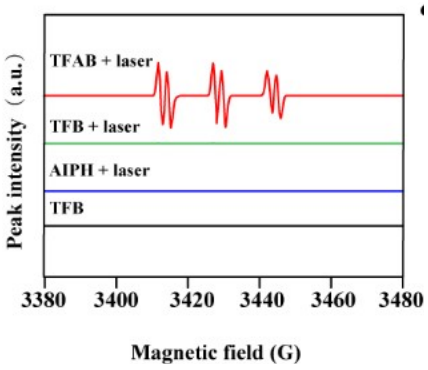

Figure S9 ESR spectra for alkyl free radical detection.

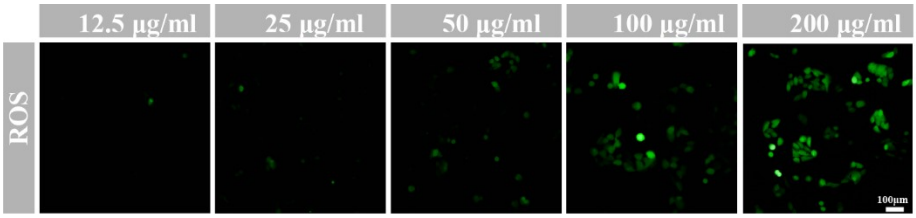

Figure S10: ROS generation at different TFAB concentrations

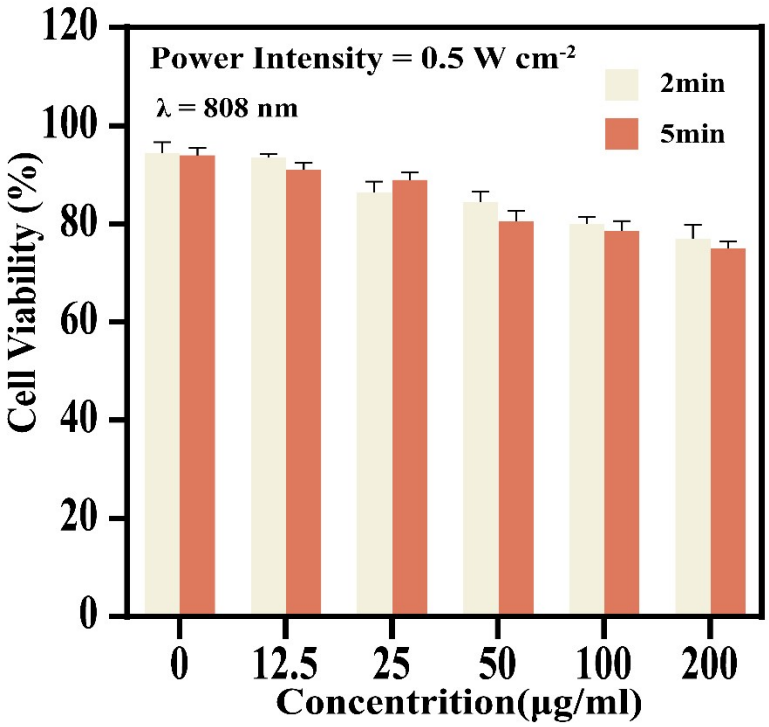

Figure S11 Relative cell viability of different concentrations (0, 12.5, 25, 50, 100, and 200 μg ml^{-1}) of TFAB NPs under 808 nm laser irradiation at the power intensity of 0.5 W cm^{-2} for 2 and 5 min.

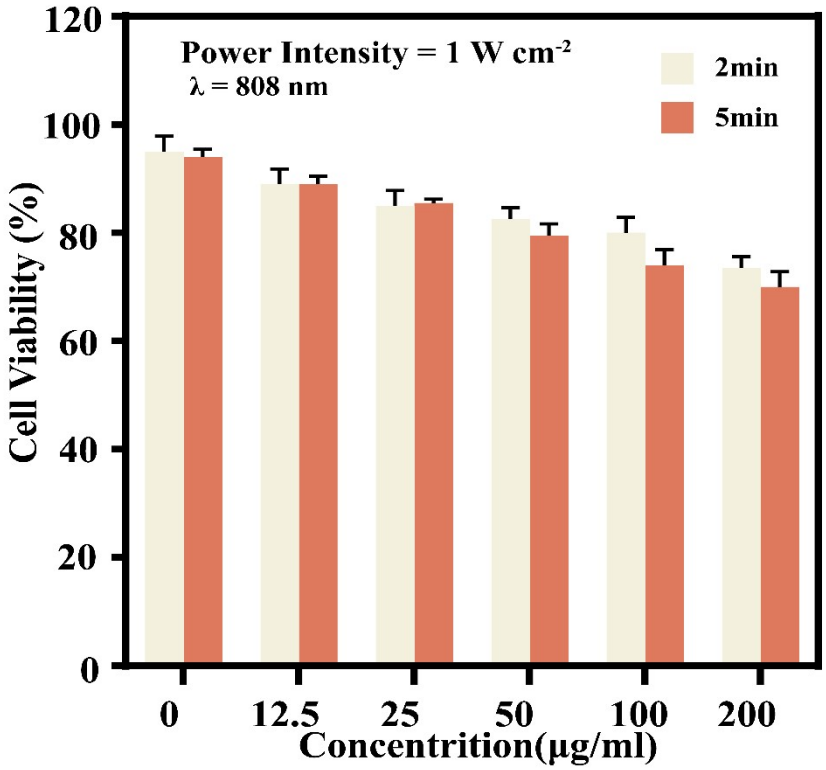

Figure S12 Relative cell viability of different concentrations (0, 12.5, 25, 50, 100, and 200 μg ml^{-1}) of TFAB NPs under 808 nm laser irradiation at the power intensity of 1 W cm^{-2} for 2 and 5 min.

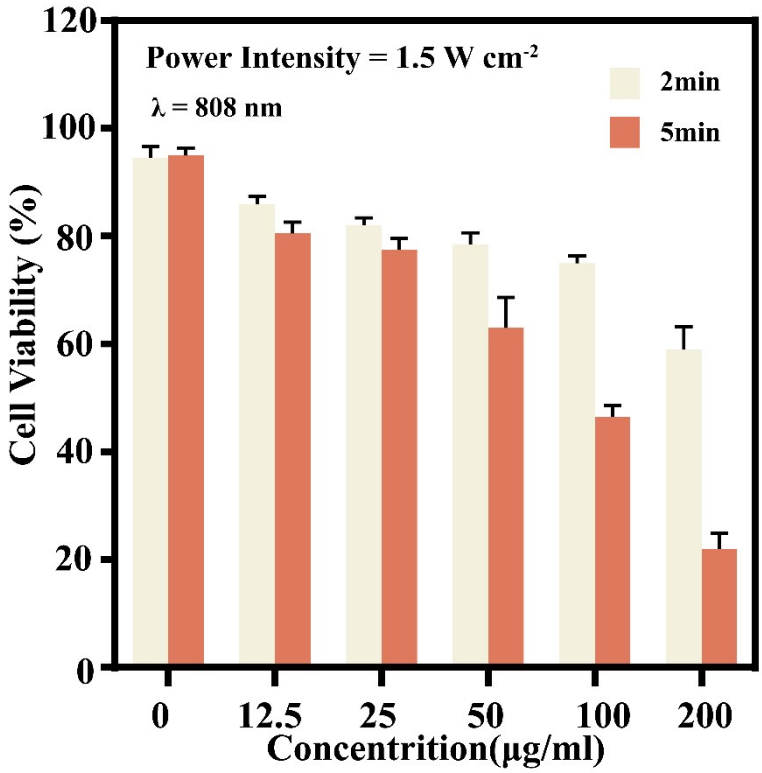

Figure S13 Relative cell viability of different concentrations (0, 12.5, 25, 50, 100, and 200 μg ml^{-1}) of TFAB NPs under 808 nm laser irradiation at the power intensity of 1.5 W cm^{-2} for 2 and 5 min.

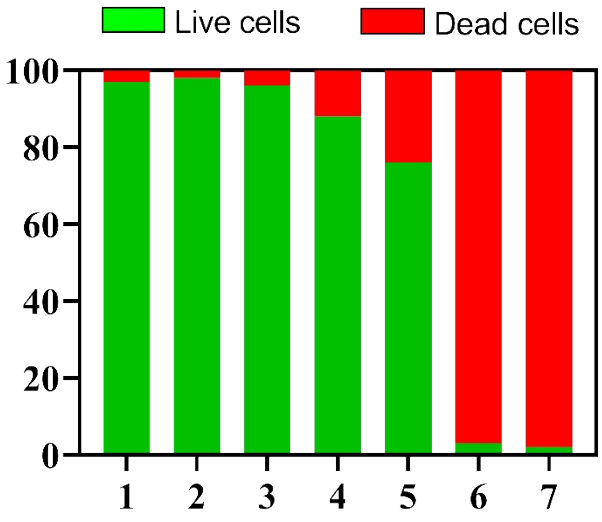

Figure S14 Statistical analysis of the apoptosis rate for MNNG/HOS cells after different treatment （1.control 2. Laser 3. AIPH + laser 4.TFB 5 TFB + laser 6 TFAB + laser （normoxia） 7.TFAB + laser （hypoixa））.

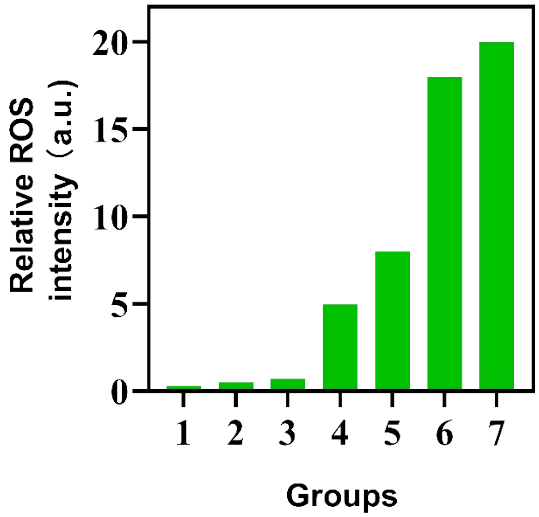

Figure S15 Corresponding quantitative data of intracellular ROS level in MNNG/HOS cells stained with DCFH-DA（1.control 2. Laser 3. AIPH + laser 4.TFB 5 TFB + laser. 6 TFAB + laser （normoxia） 7.TFAB + laser （hypoxia））.

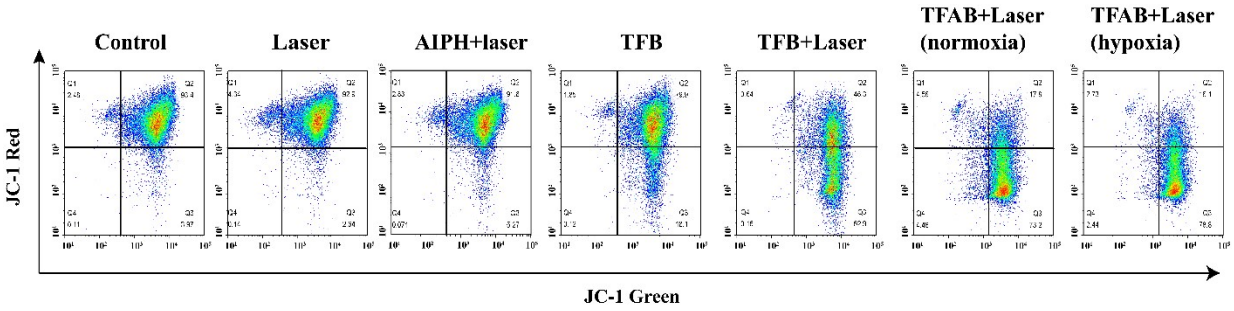

Figure S16 Flow analysis using JC-1 evaluated Mitochondrial membrane potential

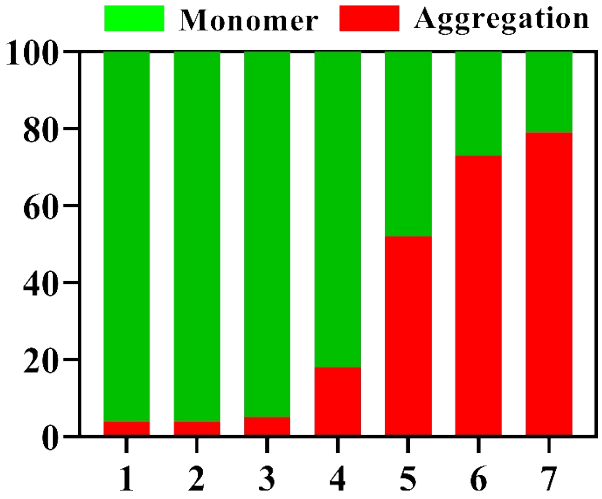

Figure S17 Green/red FL ratios of MNNG/HOS cells stained with JC-1（1.control, 2. Laser, 3. AIPH + laser, 4.TFB, 5. TFB + laser, 6. TFAB e laser （normoxia）e7.TFAB + laser （hypoxia））.

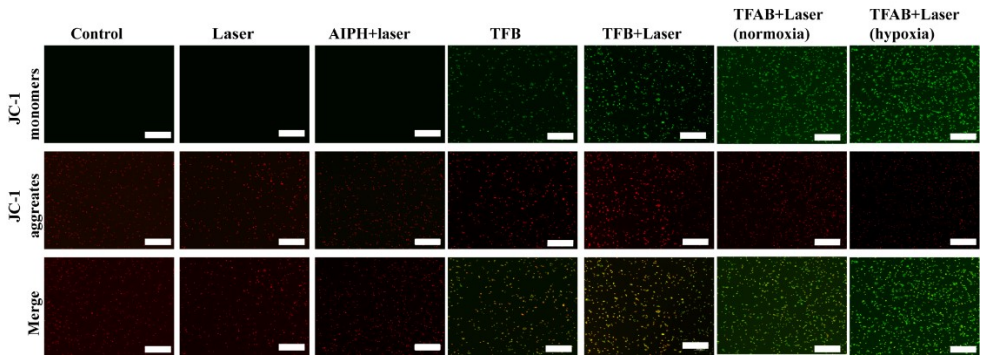

Figure S18. Confocal images of MNNG/HOS cells stained with JC-1 after different treatments （scale: 100 μm）.

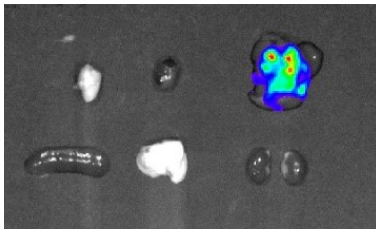

Figure S19: Fluorescence images of the tumor and excised organs 1 hour after TFAB injection.

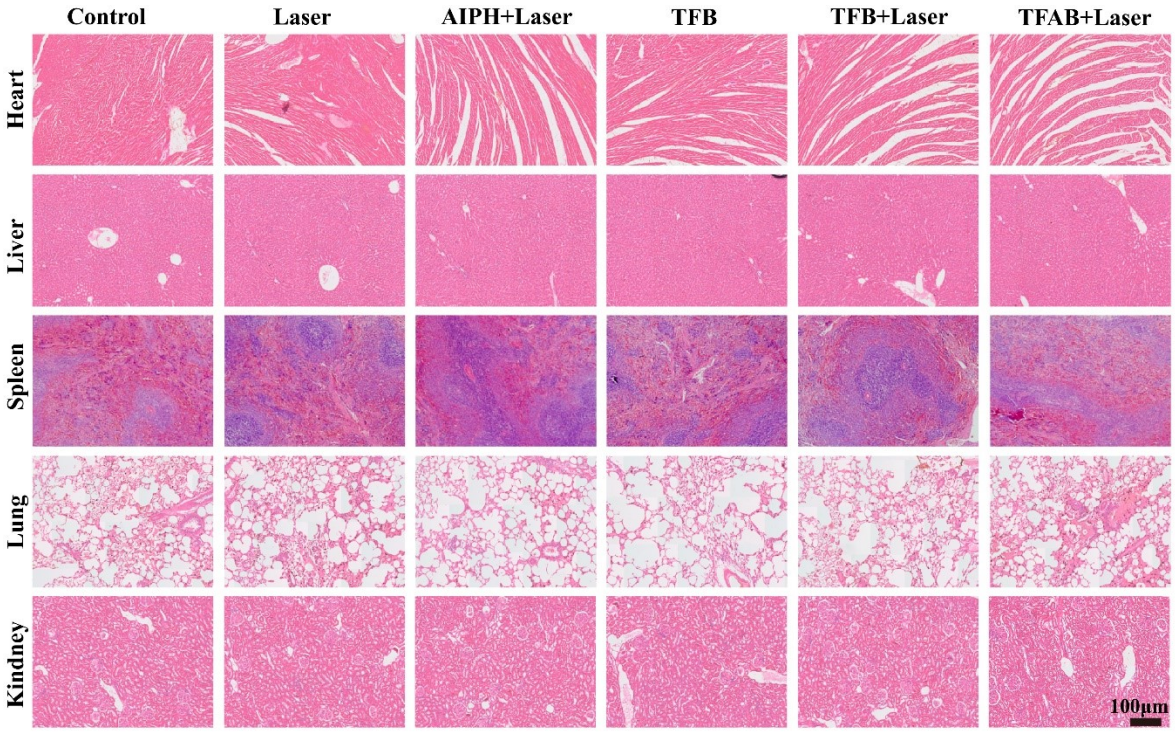

Figure S20 H&E-stained major organs (heart, liver, spleen, lung and kidney) from mice after diverse therapies on day 14（scale: 100 μm）

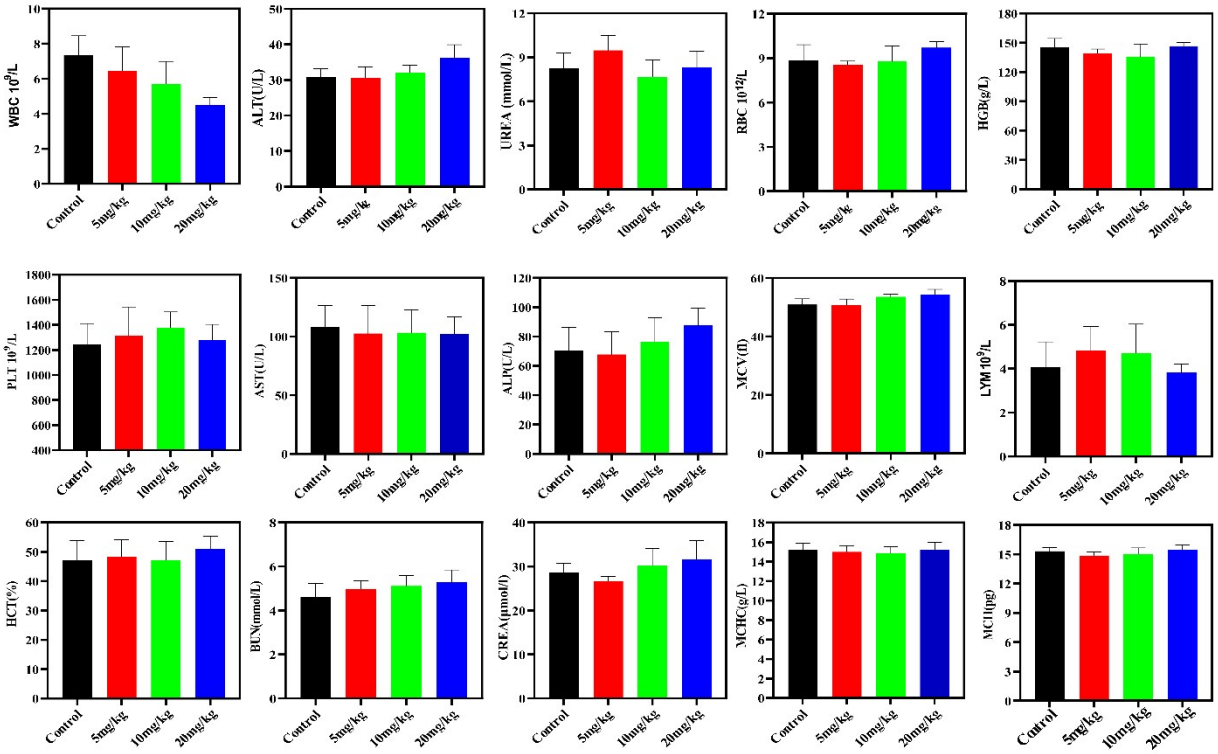

Figure S21 Blood biochemistry and hematological profiles of mice on the 14th day after intravenous injection of TFAB at different dosages.

1. R. Miao, B. Dutta, S. Sahoo, J. He, W. Zhong, S. A. Cetegen, T. Jiang, S. P. Alpay and S. L. Suib, *J Am Chem Soc*, 2017, **139**, 13604-13607.
2. Q. Li, L. Sun, M. Hou, Q. Chen, R. Yang, L. Zhang, Z. Xu, Y. Kang and P. Xue, *ACS Appl Mater Interfaces*, 2019, **11**, 417-429.